Journal Name

ARTICLE

Three dimension modelling of the components in supercapacitors for proper understanding and contribution of each parameter to the final electrochemical performance

Received 00th January 20xx,
Accepted 00th January 20xx

DOI: 10.1039/x0xx00000x

www.rsc.org/

Farshad Barzegar *[a], Lijun Zhang [a], Abdulhakeem Bello [b,c], Ncholu Manyala [b], Xiaohua Xia [a]

Abstract Three dimension (3D) modelling of supercapacitors (SCs) has been investigated for the first time to have a better understanding and study the effect of each parameter on the final electrochemical results. Based on this model, the resistance of the electrolyte, membrane, current collectors and active materials, have effect on the first intersection point on the real axis (x-axis) of the Nyquist plots (equivalent series resistance (ESR)). These results indicate inward shrinking of the cyclic voltammograms (CV) due to a small change in the leakage resistance and resistance of the faradic component of materials, it also explains the parameters that lead to the deformation of the CV from the ideal behaviour. The 3D model was verified with experiments using activated carbon-based SCs devices. The experimental results confirmed the 3D model results and suggest that the proposed 3D model is reliable and can be used for the proper design of SC devices.

Introduction

The Storage systems with sufficient capacity and highly efficient charge and discharge characteristics are of huge and strategic importance for portable electronic, biomedical applications, as well as short and medium-term stationary applications. For this purpose, different technologies are being developed including mechanical, thermal, physical, chemical and electrochemical energy storage systems [1]. Advanced solutions with high energy densities are batteries, however, they suffer from low power density, a short cycle life, safety risks and poor adaptability with flexible systems [2]. Electrochemical capacitors (ECs) also called supercapacitors with high power density, good cycling stability, and fast charge-discharge rate are a new energy storage devices that have attracted attention in the scientific community [3–5]. Currently, research in the field of supercapacitors is focused on fine-tuning electrode, electrolyte and material section to achieve the best performance [6–8]. However, there are no studies on the effect of resistances of each parameter on final electrochemical performance which can help researchers to develop and synthesize the best ECs depending on the usage.
For a better understanding of the ECs, we need to understand the full behavior of each component of the ECs during charge and discharge. Based on the charge storage mechanism, ECs can be classified as electric double layer capacitors (EDLCs), pseudo-capacitors or redox electrochemical capacitors (RECs) and hybrid electrochemical capacitors [9]. The EDLCs store energy by the charge separation at the electrode-electrolyte interface [10], while RECs materials, which not only store energy like an EDLC but also in the appropriate potential window represent electrochemical faradaic reactions between electrode materials and ions [11]. Until now most researchers have tried to explain the electrical behavior of the pure EDLCs [12] for ECs, however, none of the reports clearly explained effect and reflection of resistances of each component of the ECs on their behavior leading to the final stored energy. In this article, we study and provide a deep understanding of the electrical behavior of ECs and the effect of each component to the final electrochemical performance. The verification and confirmation of the proposed model, was carried out experimentally with activated carbon-based materials and KOH aqueous electrolyte in the laboratory.

Modelling of the Supercapacitor

The electrical behavior of ECs can be described by the lumped-element impedance-based model. The most common models for the description of EDLCs are in three categories namely; RC circuit model, three branch RC circuit model, and a transmission line model (Fig. 1). The simple RC circuit model, as shown in Fig. 1 (a), includes four ideal circuit elements, the $\mathbf{R_S}$ element presents series resistance which is due to the presence of electrolyte and the metallic conductors, **L** element presents the series inductance that is mostly influenced by the geometry of the connectors and electrodes, **C** is the ideal capacitor behavior which store energy by the charge separation at the electrode-electrolyte interface and $\mathbf{R_{CT}}$ element due to the process of charge transfer from the electrode to the electrolyte and

[a] Electrical, Electronic and Computer Engineering Department, University of Pretoria, Pretoria 0002, South Africa
[b] Physics Department, Institute of Applied Materials, SARCHI Chair in Carbon Technology and Materials, University of Pretoria, Pretoria 0028, South Africa
[c] Department of Materials Science and Engineering, African University of Science and Technology, Abuja, Nigeria
*Corresponding Author Email address: farshadbarzegar@gmail.com
*The first two authors contributed equally to this work.
Electronic Supplementary Information (ESI) available: [details of any supplementary information available should be included here]. See DOI: 10.1039/x0xx00000x

This journal is © The Royal Society of Chemistry 20xx

Please do not adjust margins

Leakage current. The loss in EDLCs energy, during self-discharge, gives rise to leakage current resistance and through charging and discharging time caused by equivalent series resistance (ESR) [13,14]. It is necessary to extend the simple RC circuit model since it cannot be used to probe porous nature of the electrodes or show the behavior of EDLCs over a frequency range accurately.

The three branch RC circuit presented by L. Zubieta and R. Bonert [15], is shown in Fig. 1 (b). It consists of the leakage resistance $\mathbf{R_{LK}}$ in parallel by three branches which correspond to different time constants for charge transfer. The first or immediate branch is for the time range of seconds and it consists of a resistance $\mathbf{R_i}$ in series with two capacitors; a voltage dependent capacitor $\mathbf{C_{i1}}$ and a normal capacitor $\mathbf{C_{i0}}$. The delayed branch with parameters $\mathbf{R_d}$ and $\mathbf{C_d}$, represents time constants within the minutes range while the long term branch, $\mathbf{R_l}$ and $\mathbf{C_l}$, represents time constants greater than ten minutes. The models show a suitable connection with experimental results, however, the models have a weakness taking into account that the circuit components lack a physical meaning [16].

The transmission line model is adopted in many reports [17,18] to represent precisely the porous nature of the electrode in EDLCs as shown in Fig. 1 (c) which includes the leakage resistance $\mathbf{R_{LK}}$, solution resistance $\mathbf{R_{el}}$, electrode resistance $\mathbf{R_{ed}}$, inductance $\mathbf{L_S}$ which is prevailing at high frequency, a resistance $\mathbf{R_P}$ that is in parallel with inductance $\mathbf{L_P}$ which are observed above resonant frequency.

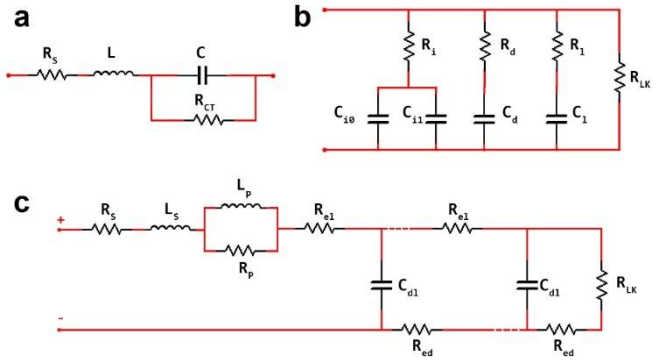

Figure 1. EDLC (a) Simple RC circuit model, (b) three RC circuit model and (c) transmission line model

All the above mentioned models are incomplete models for actual ECs and cannot be used to examine resistances of each parameter of ECs (active material, electrolyte, separator and etc.) individually and their focus is mostly on the EDLCs material. Thus, in this paper, we propose a realistic three dimensional model to study and elucidate resistances of each component of ECs individually and the influence of each component on the final behavior of ECs. Cyclic voltammetry (CV) and galvanostatic charge-discharge (GCD) modeling and measurements, cannot be completely understood in the electrochemical reaction at the electrode-electrolyte interface and a complete description can be explained by the electrochemical impedance spectroscopy (EIS) [19]. The EIS is often represented by the Nyquist plot which presents the real (x-axis) and imaginary part of the impedance (y-axis). The Nyquist plot takes into account the different parameters (resistance, capacitance, inductance and etc.) all being dependent on the frequency and is usually divided into three regions, low frequency, medium frequency and high-frequency region [20]. For an ideal capacitor, the Nyquist plot of impedance is represented by a vertical line which is parallel to the imaginary (y axis), which is only correct for liquid mercury electrode and the impedance of most solid electrodes deviates from the purely capacitive behavior [21].

To offer a realistic model close to the practical situation, the behavior of ECs should be described by a complex network of non-linear inductances, capacitors and resistances. Thus, Fig. S1 (a) and (b) have been proposed for realistic and accurate 2D model for the ideal behavior of EDLCs and RECs material respectively. The ECs shown in Fig. 2 and S1, depend on several parameters, such as the capacitor that present double layer behavior (C_1 and C_2), the capacitor that present redox electrochemical behavior (C_{F1} and C_{F2}), inductance (L), resistance of the electrolyte (R_e), current collector and electrode materials resistance (R_C), membrane resistance (R_m), Faradic part of material resistance (R_f) and leakage resistance (R_{lk}) (that is dependent on packaging). The suggested RECs model in our simulation is based on their behavior that is close to battery material [22,23], due to the fact that most oxide materials for RECs show a Faradaic phenomenon. In reality, the presence of functional groups at the surface of the electrode materials for EDLCs cannot be overruled and they show similar behavior to RECs during charge and discharge contributing a pseudo-capacitive effect to the total electrochemical performance. Similarly, some oxide materials such as RuO and MnO_2 exhibit EDLC behavior (pseudo) [24] and makes their model complex. To resolve this issue, the final 2D model presented in Fig. S1 (c) considered a hybrid model that takes care of all the functional groups and other parameters bringing the model close to the practical ECs behavior. Lastly, a 3D hybrid model in Fig. 2 (S1 (d)) was suggested for a realistic simulation of the EDLCs behavior.

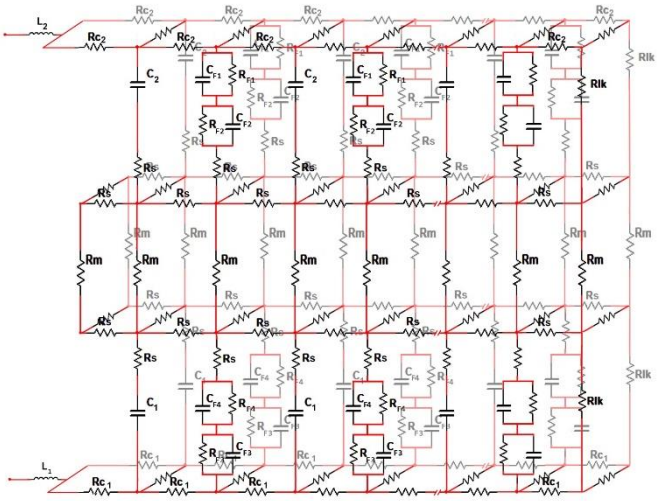

Figure 2. 3D electrical equivalent model of practical ECs

This journal is © The Royal Society of Chemistry 20xx

Please do not adjust margins

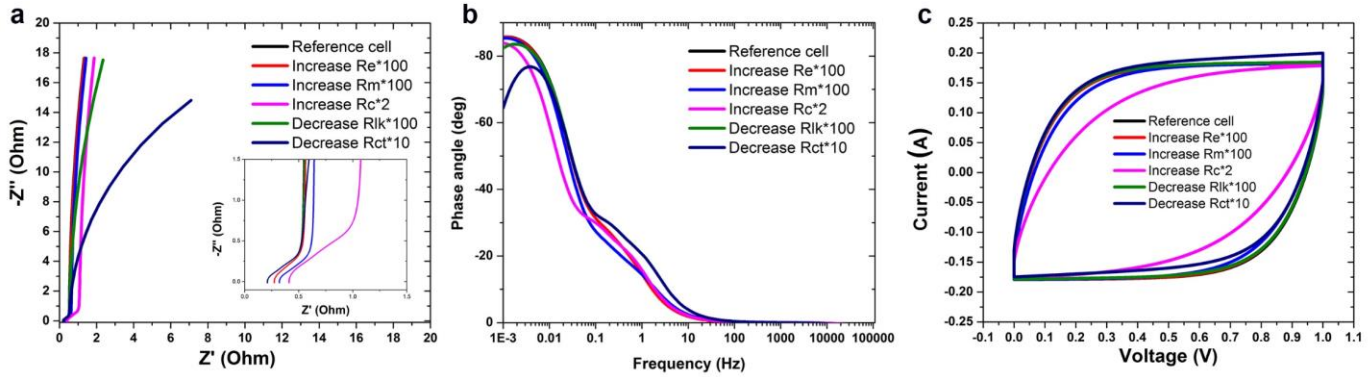

Figure 3. (a) EIS plot, (b) the phase angle versus frequency and (d) CV curves of simulation results

Methods

Simulation of the full cell supercapacitor

In order to study the performance of the passive hybrid system and to verify the analytical approach above, simulations in Matlab/Simulink is conducted using Simpower GUI. A saw tooth wave with the maximum voltage of 1 V and frequency of 0.01 is used to charge and discharge the cell in order to simulate its performance. Firstly, the 2D model is built in Simulink shown in Fig. S2. The Two 2D models in Fig. S2 are then connected together through two resistor banks, each comprising Re and Rc, to form the 3D model shown in the right hand side of Fig. S3. The left hand side of Fig. S3 shows the charge/discharge control and output voltage and current measurement circuit, where Isc.mat and Vsc.mat store the simulated current and voltage profiles of the cell and Vchg.mat provides the saw tooth voltage waveform to charge/discharge data given in Fig. S4.

Experimental and electrode preparation of the full cell supercapacitor

Polymer based activated carbon (AC) was used in experimental section and was prepared by the methods reported in our previous work [25] using hydrocarbons such as polyvinyl alcohol (PVA)/ Polyvinylpyrrolidone (PVP) as a source of carbon, through chemical activation with KOH as the active agent to produce the desired porous carbons. The porous carbon (activated carbon (AC)) that was used for the electrochemical test has surface area of 1063 m^2 g^{-1} and has some functional groups on the surface as explained in our previous work. The electrodes were made by combining the active materials, conductive additive (carbon black) and Polyvinylidene fluoride (PVDF) in N-methyl pyrrolidone (NMP) to make a slurry which was coated on a Nickel foam graphene coated as a current collector and dried at 60 °C in an oven overnight. The device was tested in a two-electrode configuration with a microfiber filter paper (thickness of 180 µm with 11 µm pore size (particle retention)) as a separator. Three set of devices were made and tested numerous times to ascertain the reproducibility before coming to the conclusion. The reference cell and first device consisted of the active material (activated carbon with functional group) derived from PVA\PVP, carbon black and PVDF with weight ratio of 90%, 5% and 5% respectively, 6 M KOH, one glass microfiber filter paper separator and graphene coated Nickel foam current collector. Furthermore, the resistance of the active material (R_C) in the second device was increased by increasing the binder by 10% without the addition of a conductive agent (carbon black). The third device was made with the intention of increasing the resistance of the electrolyte (R_e), where the 5 ml of 10 .wt% PVA solution was add to 5 ml of 6 M KOH. The number of the separators was also increased so as to slow the movement of ions with the electrodes which will result in increased membrane resistance (R_m). It's worth stating that it quit difficult to control all other parameters in reality and thus all the test parameters were repeated numerous times to confirm the results obtained. Electrochemical measurement (electrochemical impedance spectroscopy (EIS) and Cyclic voltammetry (CV)) were carried out using a Bio-logic VMP-300 potentiostat. The EIS measurements were conducted in the frequency range from 0.01 Hz to 100 kHz with the open circuit potential (~ 0 V).

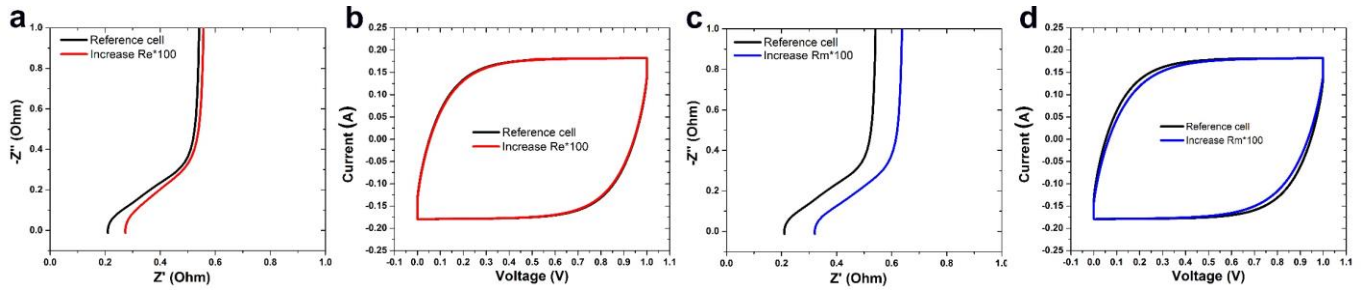

Figure 4. Simulation result of EIS plot and CV curves when (a) and (b) increasing resistance of the electrolyte 100 times, (c) and (d) increasing membrane resistance 100 times

Please do not adjust margins

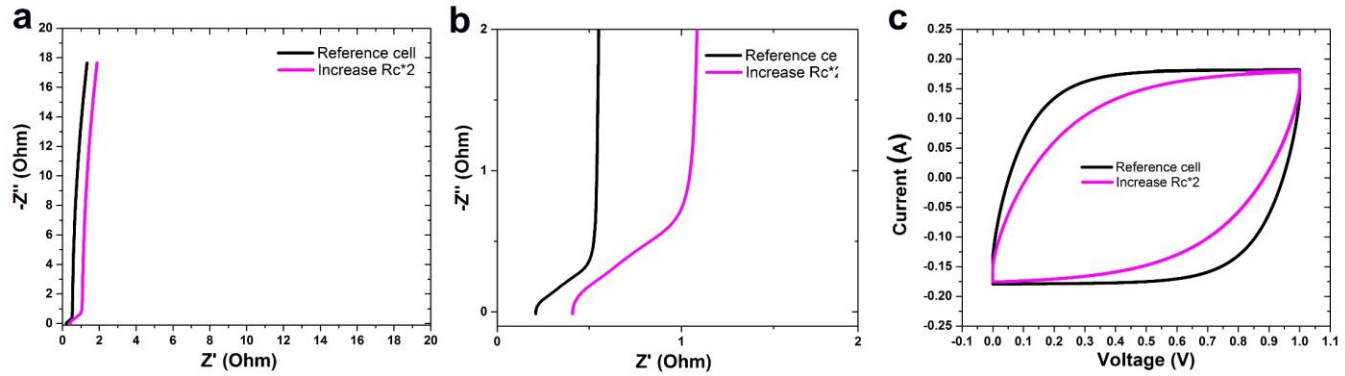

Figure 5. Simulation result of (a) and (b) EIS plot and (c) CV curves when increasing current collectors and active materials resistance 2 times

Results and Discussion

To study the effect and reflection of resistances of each parameter to the final electrochemical performance separately, the reference cell will be necessary. After the 3D model of supercapacitor designed, each parameter of the cell was assigned the specific value and the outcome of that was considered as reference cell result. Then, to study parameters effect individually, each parameter was changed separately when the rest of the parameters were fixed with reference amount. To see the negative effect of each parameter compare to the reference cell, some of the parameters were increased and some were decreased. The modified value is just a number that it's high enough to see the effect of each parameter compared to reference cell. Fig. 3 displays the EIS plot, the phase angle versus frequency and CV curves of simulation results after changing resistance of each parameter compared to reference cell. In our simulation results, R_e represents the resistance of the electrolyte, R_m is the resistance of membrane, R_c is a resistance of current collector and electrode materials, R_{lk} is leakage resistance and R_{ct} is the resistance of the Faradic part of the material. It is clear that each parameter has a different effect on the final result of the supercapacitor. For better understanding and clarity of the result, each parameter is plotted and investigated separately compared to reference cell.

Fig. 4 (a) and (b) presents the effect of the electrolyte resistance on the final results of EIS plot and CV curves. As observed from Fig. 4 (a) change in the resistance of the electrolyte (R_e) by a factor of 100 lead to an increase in the first intersection points on the real axis (x-axis) of the Nyquist plots. This frequency plot corresponds to typical time constants in most high-power applications, For intermediate frequencies, the complex-plane plots form an angle of ~45 with the real axis as seen in the figure. This angle is explained by the limited current penetration into the porous structure of the electrodes [26]. For lower frequencies, the spectra approach a nearly vertical line in the complex plane, which is typical of ideal capacitors. Similarly, a shift and increase in the high-frequency area and the angle of Nyquist plots for the intersection of the high and medium-frequency region was also observed. The model is a highly dynamic load at the beginning as well as deeper charging and discharging. The corresponding CV and the calculated data show excellent agreement. Figure 4 (b) shows CV curves of the simulated results based on the reference cell and the simulated cell after the R_e was increased by 100 times indicating that there was no change in the shape of the CV rather a small decrease in current was observed which correspond to slight shrinkage of the CV. This also shows a decrease in the capacitance of the device.

Several other components contribute to the overall performance of the device such as the membranes that prevent short-circuiting within the device. Fig. 4 (c) and (d) presents the effect of the membrane (separator) resistance on the final performance of the device. Fig. 4 (c) shows an increase in the resistance of the membrane (R_m) by a factor of 100 show the first intersection points on the real axis (x-axis) of the Nyquist plots increased and the whole plots shift by the same length. The angle of Nyquist plots for the intersection of the high and medium-frequency region didn't change. The corresponding CV in Fig. 4 (d) shows a similar result with shrunk CV indicating a capacitive decrease. It is clear that the results obtained using the proposed model give a similar result to what is obtainable

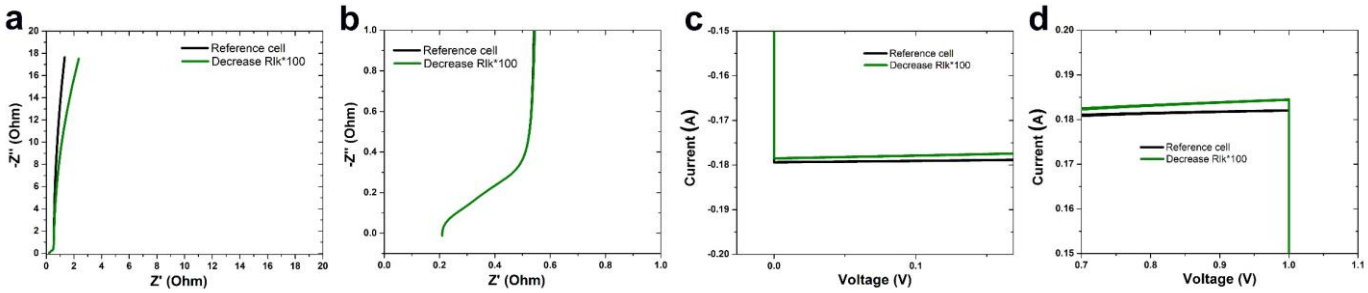

Figure 6. Simulation result of (a) and (b) EIS plot and, (c) and (d) CV curves when decreasing leakage resistance 100 times

 This journal is © The Royal Society of Chemistry 20xx

Please do not adjust margins

Please do not adjust margins

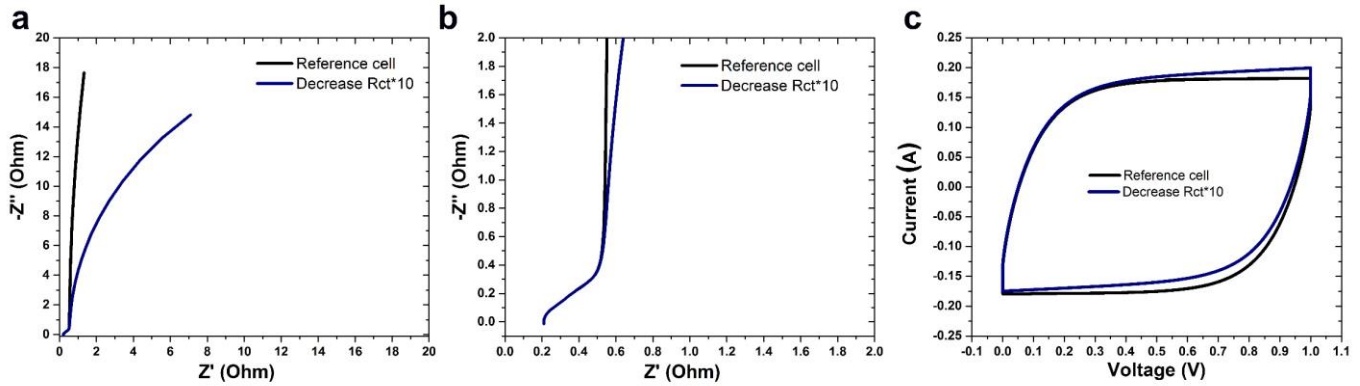

Figure 7. Simulation result of (a) and (b) EIS plot and (c) CV curves when decreasing resistance of Faradic part of material 10 times

in the experiments that is presented at the end of the paper. Therefore, the proposed electric model can be used in designing a voltage controller and in sizing a supercapacitor for storage application.

The resistance of the current collectors and active materials (and resistance at the interface of them) also play a crucial part in the performance of the devices. Such contributions are presented in Fig. 5. Fig. 5 (a) and (b) shows result of increasing the resistance of the current collector and electrode materials (R_c) by a factor of 2 (The parameter that was chosen for R_c for reference cell was high at first, so increase by a factor of 2 making it high enough to see the effect of R_c compare to reference cell). From Fig. 5 (b) which provides an enlarged view of the Nyquist plot, showing remarkable deviations attributed to the longer time that charge can reach to the surface of the active material. This deviation could also affect the efficiency of the device which is influenced by the resistance of the electrodes which means that increasing the real part of the impedance with a corresponding decrease in frequency has to be taken into consideration. However, the angle of Nyquist plots for the intersection of the high and medium-frequency region remained the same. Fig. 5 (c) shows a clear shrinkage in the CV that explains a decrease in the performance of the device, hinting that the resistance of active material and current collector play a crucial part in the performance of the electrochemical devices. The shrinking might be attributed to a number of factors such as the, the conductivity, the pore dimension of the active materials and current collectors.

Fig. 6 presents the effect of leakage resistance (R_{lk}) on the final results. Figure 6 (a) and (b) show that by decreasing the R_{lk} by 100 times, the first intersection points on the real axis (x-axis) of the Nyquist plots didn't change. Decreasing the R_{lk} put a negative effect on the capacitance of the supercapacitor. The only part affected is the low-frequency region that shows more deviation from the vertical lines. Decreasing the R_{lk} means that the cell has an easier way to discharge than keeping the charge at the surface. Fig. 6 (c) and (d) shows CV curves of a simulation result of the reference cell and the cell after decreasing R_{lk} by 100 times. For the first time, this paper reports an upward shift and shape change (pushed inward) of the CV curve by adjusting one parameter such as leakage resistance (Fig. 6) or resistance of the Faradic part of materials (effect of functional group) (Fig. 7). The initial and final point moved up and the shape of CV curves pushed inward a little. The shift in CV is more at the endpoint with high current than the first point with the low current which is considered as a shift to match the initial point. As EIS results showed, that decreasing the R_{lk} put a negative effect on the capacitance of the supercapacitor, thus, by decreasing the R_{lk}, supercapacitor needs more energy to charge than the energy given on discharge section.

Fig. 7 presents the effect of the resistance of the Faradic part of the material (R_{ct}) on final results. As shown in Fig. 7 (a) and (b), a decrease in the R_{ct} by 10 times leads to no change in the intercept value on the real axis (x-axis) of the Nyquist plots, however, it introduces a negative effect on the Faradic part of the supercapacitor performance. The only part that gets affected is the low-frequency region that becomes more resistive and deviate from the vertical lines. Fig. 7 (c) shows CV curves of a simulation result of the reference cell and the cell after decreasing R_{ct} by 10 times. It shows the same trend as Fig 6 (c) and (d). The initial and final point moved up and the shape of CV curves pushed inward a little. Decrease in the R_{ct} reduce the potential capacity of the capacitor that present redox electrochemical behavior (C_F) and put a negative effect on the capacitance of the supercapacitor so that ECs need more energy to charge than the energy given on discharge section. The R_{ct}

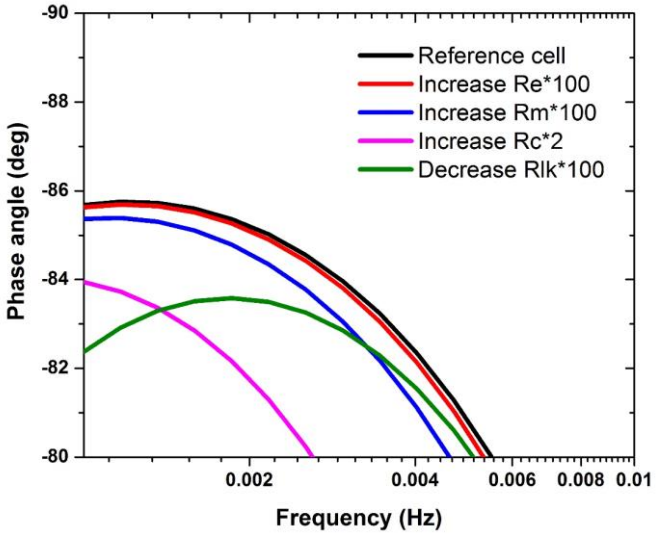

Figure 8. An enlarged view of the phase angle versus frequency of the simulations

Please do not adjust margins

Please do not adjust margins

and C_F have a very close relationship to each other that linked to the material properties.

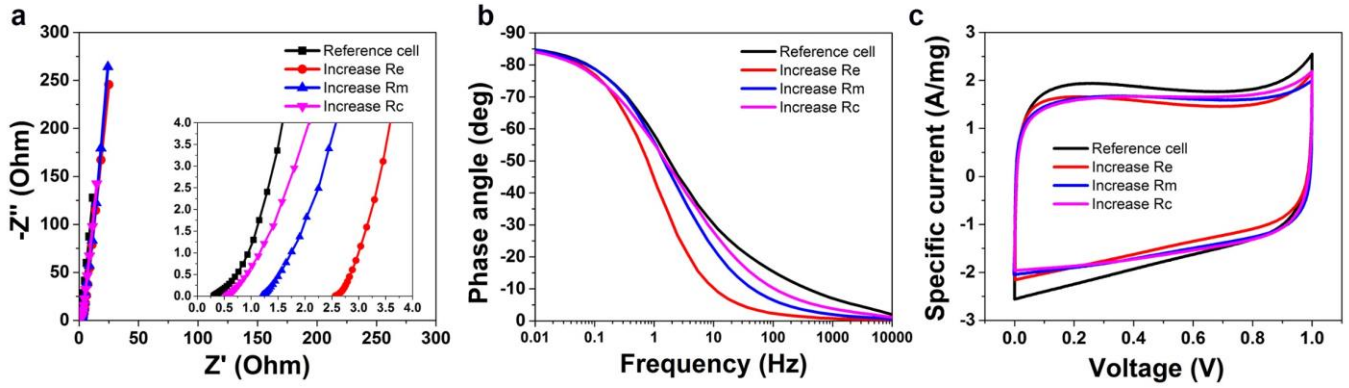

Figure 9. (a) EIS plot, (b) the phase angle versus frequency and, (c) CV curves at scan rates of 20 mV $^{s-1}$ of material in reality

Fig. 8 presents an enlarged view of the phase angle versus frequency of the simulations. This figure shows the effect of each parameter discussed above on the final result of the phase angle. The ideal capacitor phase angle should be −90°. The closer the phase angle is to −90° means the device performs similar to an ideal capacitor [27]. Fig. 8 shows the same trend that all EIS simulation showed similar trend. Those parameters that put a more resistive behavior on final capacity, moves far away from the -90°.

For the purpose of verifying the analysis above and confirming the proposed model, experiments with the activated carbon-based supercapacitor were tested in the laboratory. In the experimental section the parameters that are possible to control physically in our laboratory were investigated. The investigation of the high-frequency region and effect of each resistive component of the device was carried out experimentally to ascertain and confirm the proposed three-dimensional hybrid model. We detected the same trend in Fig. 9 as the 3D simulation results proposed. However, as shown in Fig. 9 (a), the length of the EIS increased after changing one parameter due to the fact that the mass of the material is not completely as uniform as reference cell and the other cell. Controlling the mass in such scale is very difficult with our equipment. The phase angle (Fig 9 (b) and Fig S5) and CV curves (Fig 9 (c)) of the experimental were also followed the 3D model results that suggest the proposed model was completely correct. By conniving the mass effect on capacity, the CV shape after increasing the R_e is almost the same as reference cell. Increasing the R_m and R_c, clear shrinkage occurs in the CV shape as 3D model suggested too.

Conclusion

In conclusion, a novel 3D model of the supercapacitor was presented. The results report the effect of each parameter individually for the first time in electrochemical capacitors. Based on the proposed 3D model, the resistance of the electrolyte, membrane resistance, current collectors and active materials resistance can increase the first intersection points on the real axis (x-axis) of the Nyquist plots. Also, the results revealed a novel phenomenon when the initial and final point of the CV curves shifts up and the shape of CV curves pushed inward a little by changing the leakage resistance and resistance of the Faradaic part of materials. These can explain which parameters play a major role in deformation of the CV shape from the ideal state. The experimental results confirmed that the proposed is completely correct, in that the change of any of the aforementioned parameters indeed increase the first intersection point on the x-axis of the Nyquist plot and also affect the shape of the CV curves. To improve the ECs performance based on the reported results, the selected electrolyte should have highest ionic conductivity, the chosen membrane should have sufficient size of porosity base on the electrolyte to get lowest ionic resistivity, the current collector should have the highest conductivity with good surface interaction with the active material and the active material should have highest electrical conductivity. The leakage resistance dependents on the packaging of the cell, so packaging method plays an important role in the final result. Finally, the Faradaic part of the active material can improve the capacity of the ECs by choosing the best candidate with high capacitance and low resistive behaviour (if R_{ct} is high in the material, it acts as capacity with low resistive behaviour).

Conflicts of interest

There are no conflicts to declare.

Acknowledgements

This research is co-sponsored by the National Research Foundation of South Africa (Grant Number: 61056). All findings, conclusion or recommendation expressed in this work are solely that of the author(s). The NRF does not accept liability in any regard.

References

1 H. Ibrahim, A. Ilinca and J. Perron, *Renew. Sustain. Energy Rev.*, 2008, **12**, 1221–1250.

2 C. Shen, Y. Xie, B. Zhu, M. Sanghadasa, Y. Tang and L. Lin, *Sci. Rep.*, 2017, **7**, 14324.

3 P. Simon and Y. Gogotsi, *Nat. Mater.*, 2008, **7**, 845–854.

This journal is © The Royal Society of Chemistry 20xx

Please do not adjust margins

Please do not adjust margins

4 J. Pu, F. Cui, S. Chu, T. Wang, E. Sheng and Z. Wang, *ACS Sustain. Chem. Eng.*, 2014, **2**, 809–815.

5 H. Jiang, P. S. Lee and C. Li, *Energy Environ. Sci.*, 2013, **6**, 41–53.

6 F. Barzegar, A. Bello, J. K. J. K. Dangbegnon, N. Manyala and X. Xia, *Appl. Energy*, 2017, **207**, 417–426.

7 F. Barzegar, J. K. J. K. Dangbegnon, A. Bello, D. Y. D. Y. Momodu, A. T. C. T. C. Johnson and N. Manyala, *AIP Adv.*, 2015, **5**, 097171.

8 Y. Wang, Y. Song and Y. Xia, *Chem. Soc. Rev.*, 2016, **45**, 5925–5950.

9 F. Wang, X. Wu, X. Yuan, Z. Liu, Y. Zhang, L. Fu, Y. Zhu, Q. Zhou, Y. Wu and W. Huang, *Chem. Soc. Rev.*, 2017, **46**, 6816–6854.

10 T. Purkait, G. Singh, D. Kumar, M. Singh and R. S. Dey, *Sci. Rep.*, 2018, **8**, 640.

11 D. W. Lee, J. H. Lee, N. K. Min and J.-H. Jin, *Sci. Rep.*, 2017, **7**, 12005.

12 B.-A. Mei and L. Pilon, *Electrochim. Acta*, 2017, **255**, 168–178.

13 A. B. Cultura and Z. M. Salameh, 2015, 876–882.

14 O. Bohlen, J. Kowal and Dirk Uwe Sauer, *J. Power Sources*, 2007, **173**, 626–632.

15 L. Zubieta and R. Bonert, *IEEE Trans. Ind. Appl.*, 2000, **36**, 199–205.

16 N. Ber, J. Sabatier, O. Briat and J.-M. Vinassa, *IEEE Trans. Ind. Electron.*, 2010, **57**, 3991–4000.

17 W. Lajnef, J.-M. Vinassa, O. Briat, S. Azzopardi and E. Woirgard, *J. Power Sources*, 2007, **168**, 553–560.

18 A. Hammar, P. Venet, R. Lallemand, G. Coquery and G. Rojat, *IEEE Trans. Ind. Electron.*, 2010, **57**, 3972–3979.

19 S.-M. Park and J.-S. Yoo, *Anal. Chem.*, 2003, **75**, 455 A-461 A.

20 M. E. Orazem and B. Tribollet, *Electrochemical Impedance Spectroscopy*, John Wiley & Sons, 2011.

21 H.-K. Song, H.-Y. Hwang, K.-H. Lee and L. H. Dao, *Electrochim. Acta*, 2000, **45**, 2241–2257.

22 H. He, R. Xiong and J. Fan, *Energies*, 2011, **4**, 582–598.

23 A. Rahmoun, H. Biechl and A. Rosin, *Electr. Control Commun. Eng.*, 2013, **2**, 34–39.

24 Z. J. Han, D. H. Seo, S. Yick, J. H. Chen and K. Ostrikov, *NPG Asia Mater.*, 2014, **6**, e140–e140.

25 F. Barzegar, A. Bello, O. O. Fashedemi, J. K. Dangbegnon, D. Y. Momodu, F. Taghizadeh and N. Manyala, *Electrochim. Acta*, 2015, **180**, 442–450.

26 S. Buller, E. Karden, D. Kok and R. W. De Doncker, in *Thirty-sixth IAS annual meeting*, IEEE, 2001, vol. 4, pp. 2500–2504.

27 K. Sheng, Y. Sun, C. Li, W. Yuan and G. Shi, *Sci. Rep.*, 2012, **2**, 247.

This journal is © The Royal Society of Chemistry 20xx

Please do not adjust margins